DESY 09-132
DCPT/09/124
IPPP/09/62

arXiv:0909.0649v1 [astro-ph.CO] 3 Sep 2009

DESY 09-132; DCPT/09/124; IPPP/09/62

Late time CMB anisotropies constrain mini-charged particles

C Burrage[1], J Jaeckel[2], J Redondo[1] and A Ringwald[1]

[1] Deutsches Elektronen Synchrotron DESY, Notkestrasse 85, D-22607 Hamburg, Germany

[2] Institute for Particle Physics and Phenomenology, Durham University, Durham, DH1 3LE, UK

E-mail: clare.burrage@desy.de; joerg.jaeckel@durham.ac.uk; javier.redondo@desy.de; andreas.ringwald@desy.de

Abstract. Observations of the temperature anisotropies induced as light from the CMB passes through large scale structures in the late universe are a sensitive probe of the interactions of photons in such environments. In extensions of the Standard Model which give rise to mini-charged particles, photons propagating through transverse magnetic fields can be lost to pair production of such particles. Such a decrement in the photon flux would occur as photons from the CMB traverse the magnetic fields of galaxy clusters. Therefore late time CMB anisotropies can be used to constrain the properties of mini-charged particles. We outline how this test is constructed, and present new constraints on mini-charged particles from observations of the Sunyaev-Zel'dovich effect in the Coma cluster.

1. Introduction

Precision measurements of the Cosmic Microwave Background (CMB) radiation have, in recent years, enormously advanced our understanding of the origins, content and structure of our universe. Measurements of secondary anisotropies induced, not at the surface of last scattering ($z \approx 1100$), but in the more recent universe ($z \sim \mathcal{O}(1)$) also provide detailed information about the late time evolution of the universe enabling, for example, measurements of the Hubble constant through the Sunyaev-Zel'dovich (SZ) effect (for a review see [1]), and measurements of the properties of dark energy through the late time Integrated Sachs-Wolfe effect (ISW) [2, 3].

These precision measurements can also be used to test 'new physics', including the existence of new light, weakly interacting particles if they influence the propagation of photons. In this article we focus in particular on mini-charged particles (MCPs). MCPs are particles with a small and not necessarily quantized charge. Such particles arise naturally in extensions of the Standard Model which contain at least one additional U(1) hidden sector gauge group [4, 5]. The gauge boson of this additional U(1) is known as a hidden photon, and hidden sector particles, charged under the hidden U(1) get an induced electric charge proportional to the small mixing angle between the kinetic terms of the two photons. In string theory such hidden U(1)s and the required kinetic mixing are a generic feature [6–14]. Hidden photons are not *necessary* however to explain mini-charged particles, and explicit brane world scenarios have been constructed [15] where MCPs arise without the need for hidden photons.

The existence of MCPs would lead to the decay of photons in the presence of electric or magnetic fields [16, 17]. This has lead to searches for MCPs in high precision optical experiments (BFRT [18], PVLAS [19], Q&A [20], BMV [21] and OSQAR [22]) where a laser beam is passed through a transverse magnetic field and the real and virtual production of MCPs leads to rotation and ellipticity of the polarization of the beam. This signal differs depending on whether or not the model under examination includes hidden photons. In addition the presence of hidden photons can lead to more exotic effects, such as light-shining-through-walls [23, 24].

For a wide range of parameters, however, more stringent constraints on MCPs come from observations in astrophysics and cosmology [25, 26]. In particular extensions of the Standard Model which include MCPs must be in agreement with the bounds of Big Bang Nucleosynthesis (BBN), and must not lead to overly fast cooling of white dwarf and red giant stars. However it has been shown [27] that in models containing more than one hidden photon, where at least one of the hidden photons is massless, the bounds obtained in settings with high density/temperature can be considerably relaxed. Most prominently this affects bounds from energy loss considerations in stars. Therefore alternative constraints obtained in low density/temperature environments are of particular interest [28, 29]. For this we turn to observations of the CMB; the light we observe from the CMB has traveled solely through low density/temperature environments, and therefore constraints on MCPs derivable from the CMB also apply to those models which avoid the stellar evolution bounds. These constraints would be of direct relevance for upcoming laboratory searches

for MCPs which are typically performed under vacuum conditions. The light from the CMB passes through magnetic fields in the neighborhood of galaxy clusters, where real and virtual MCPs are produced exactly as in laboratory experiments. The anisotropies induced by such interactions contribute to the standard late time CMB anisotropies. In this article we show that observations of these effects can be used to constrain new regions of the MCP parameter space.

Cluster magnetic fields are well understood on distance scales at which the SZ effect dominates over the ISW effect, but little is known about magnetic fields in the largest structures in the universe. Therefore in this article we mainly focus on an MCP contribution to the SZ effect. When photons from the CMB pass through galaxy clusters there is a small probability that they will interact with an energetic electron in the plasma of the intracluster medium. If this happens the photons can be Thomson scattered up to higher energies, distorting the CMB spectrum. This is the Sunyaev-Zel'dovich (SZ) effect [30,31]. The temperature distortions induced in the CMB have the form

$$\frac{\Delta T}{T} = f\left(\frac{\omega}{T_{CMB}}\right)\int \frac{n_e T_e \sigma_T}{m_e}\, dl, \tag{1}$$

where $\omega = 2\pi\nu$ is the photon energy, T_{CMB} the CMB temperature, n_e the electron number density in the plasma, T_e the electron temperature, σ_T the Thomson scattering cross section and m_e the mass of the electron‡. The function $f(x)$ describes the frequency dependence of the SZ effect and in the non-relativistic and Rayleigh-Jeans ($\omega \ll T$) limits $f(x) \to -2$. The integral is along a line of sight through a cluster. A typical galaxy cluster is expected to induce temperature anisotropies of the order 10^{-4} in the CMB spectrum. Photons are lost in the long wavelength part of the CMB spectrum $\nu \lesssim 218$ GHz and there is an increase in the power of the spectrum at higher frequencies. There are now a large number of high quality measurements of the SZ effect for a variety of clusters. The physics of the SZ effect is reviewed in [32] and the current observations are reviewed in [33].

Constraints on MCPs from observations of the CMB have also been derived from processes where two CMB photons annihilate into two MCPs [28] and in the region of parameter space where MCPs do not decouple from the acoustic oscillations of the baryon-photon plasma at recombination [34]. Other cosmological probes of MCPs have also been considered, including their effect on the propagation of light from type Ia supernovae [29]. Modifications of the SZ effect by chameleonic axion-like-particles have also been discussed [35].

The outline of this article is as follows. In Section 2 we describe the effect of MCPs on the propagation of photons through magnetic fields. We solve the equations of motion and compute the survival probability for photons. In Section 3 we show how measurements of the SZ effect can be used to constrain MCPs, in Section 3.1 we give the constraints on MCP models that come from observations of the Coma cluster and in Section 3.2 we discuss the relevance of these constraints to hyperweak gauge interactions in the LARGE volume scenario of string theory. Section 4 describes how, in the future, observations of the ISW effect may also be used to constrain MCPs, and we conclude in Section 5.

‡ We are using units $k_B = \hbar = c = 1$.

2. Optics with MCPs and hidden photons

Photon propagation in the presence of mini-charged particles can be studied in the Holdom model [4] starting with the most general Lagrangian

$$\mathcal{L} = -\frac{1}{4}\tilde{F}_{\mu\nu}\tilde{F}^{\mu\nu} - \frac{1}{4}\tilde{B}_{\mu\nu}\tilde{B}^{\mu\nu} - \frac{\sin\chi}{2}\tilde{B}_{\mu\nu}\tilde{F}^{\mu\nu} + \tilde{e}j^{\mu}_{\rm em}\tilde{A}_{\mu} + e_h j^{\mu}_{\rm h}\tilde{B}_{\mu}, \tag{2}$$

describing visible sector photons $\tilde{A}_\mu$, hidden sector photons $\tilde{B}_\mu$, and visible and hidden sector matter fields, written here as the currents $j^\mu_{\rm em}$ and $j^\mu_{\rm h}$ respectively. The visible and hidden photons have field strength tensors $\tilde{F}_{\mu\nu}$ and $\tilde{B}_{\mu\nu}$ respectively, and χ controls the strength of the kinetic mixing between the photon fields. The visible and hidden sector gauge couplings are $\tilde{e}$ and e_h.

The following change of variables

$$\tilde{A} = \frac{1}{\cos\chi}A \quad ; \quad \tilde{B} = B - \tan\chi A, \tag{3}$$

diagonalizes the kinetic part of the Lagrangian, which can then be written as

$$\mathcal{L} = -\frac{1}{4}F_{\mu\nu}F^{\mu\nu} - \frac{1}{4}B_{\mu\nu}B^{\mu\nu} + ej^{\mu}_{\rm em}A_{\mu} + e_h j^{\mu}_{\rm h}B_{\mu} + \epsilon e j^{\mu}_{\rm h}A_{\mu}, \tag{4}$$

with $\epsilon = (e_h/e)\tan\chi$ and $e = \tilde{e}/\cos\chi$. The last term of (4) gives an effective charge under the visible sector gauge group to the hidden matter. If either χ or $e_{\rm h}$ are small the effective charge of the hidden matter has a naturally small value $|\epsilon| \approx e_h\chi/e \ll 1$.

In the presence of a strong transverse magnetic field the hidden matter contributes to the refraction and absorption coefficients of photons and hidden photons [16] through the complex refractive index, $\epsilon^2 e^2 \Delta N_i(\epsilon e\mathbf{B}, m_\epsilon) = \epsilon^2 e^2(\Delta n_i + i\frac{1}{2\omega}\kappa_i) = n_i - 1$, for a photon of frequency ω and an MCP with mass m_ϵ. $i = \perp, \parallel$ labels the photons polarized parallel and perpendicular to the direction of the magnetic field. The real parts, Δn_i, are the refractive indices and the imaginary parts, κ_i, are the absorption coefficients due to the production of MCPs. Full expressions for ΔN_i are given in Refs. [16,17,36,37]. The equations of motion derived from the Lagrangian (4) are

$$\left[(\omega^2 + \partial_z^2)\begin{pmatrix} 1 & 0 \\ 0 & 1 \end{pmatrix} - \begin{pmatrix} \omega_{\rm P}^2 + \mu^2\chi^2 & -\mu^2\chi \\ -\mu^2\chi & \mu^2 \end{pmatrix}\right]\begin{pmatrix} A \\ B \end{pmatrix} = 0, \tag{5}$$

where we have defined

$$\mu^2 = -2\omega^2 e_h^2 \Delta N_i \tag{6}$$

and $\tan(\chi) \to \chi$. $\omega_{\rm P}^2 = 4\pi^2\alpha n_e/m_e$ is the plasma frequency depending on the fine structure constant, the mass of an electron, m_e, and the number density, n_e, of free electrons in a plasma. The effective mass μ, normalized by the MCP mass, depends only on the polarization of the light and on the adiabatic parameter

$$\lambda = \frac{3}{2}\frac{\omega}{m_\epsilon}\frac{\epsilon e B}{m_\epsilon^2}. \tag{7}$$

The dependence of μ^2/m_ϵ^2 on λ is shown in Figure 1.

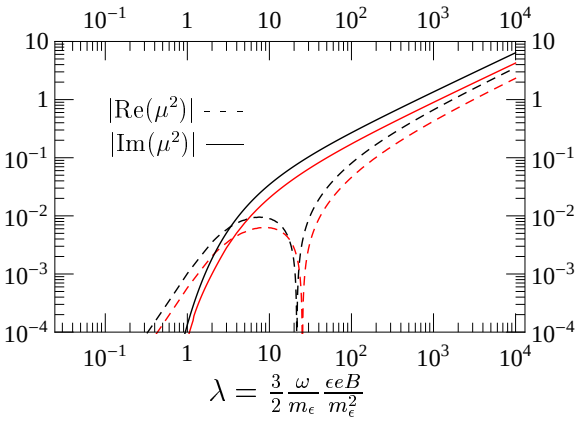

Figure 1. The absolute value of the real (solid) and imaginary (dashed) parts of the MCP-induced mass μ^2 are shown for photon polarization parallel (black) and perpendicular (red) to the magnetic field direction. The MCP particle is a Dirac spinor with mass m_ϵ and electric charge ϵ. The scalar case is very similar. They only depend on the adiabatic parameter λ. The imaginary part of μ^2 is always negative while the real part is negative for $\lambda \lesssim 20$ and becomes positive for larger values.

Solving the equations of motion, the propagating eigenstates are

$$V_+(t,z) = \begin{pmatrix} 1 \\ -a \end{pmatrix} e^{i(\omega t - k_+ z)} \quad ; \quad V_-(t,z) = \begin{pmatrix} a \\ 1 \end{pmatrix} e^{i(\omega t - k_- z)}, \tag{8}$$

where the momenta are

$$k_\pm \quad = \sqrt{\omega^2 - m_\pm^2} \simeq \omega - \frac{m_\pm^2}{2\omega} \equiv \omega - \Delta_\pm, \tag{9}$$

$$2m_\pm^2 = \omega_\mathrm{P}^2 + \mu^2(1+\chi^2) \pm \sqrt{(\omega_\mathrm{P}^2 - \mu^2(1-\chi^2))^2 + 4\mu^4\chi^2}, \tag{10}$$

and

$$a = \frac{\mu^2}{m_+^2 - \mu^2}\chi. \tag{11}$$

Therefore a state which is purely photon-like initially at $z = 0$ evolves as

$$V(t,z) = \left(\frac{1}{1+a^2} V_+(0,0) e^{i\Delta_+ z} + \frac{a}{1+a^2} V_-(0,0) e^{i\Delta_- z} \right) e^{i\omega(t-z)}. \tag{12}$$

The photon survival amplitude is the first component of this vector and, from this, the photon survival probability is

$$P_{\gamma\to\gamma}(z) = \left| \frac{1}{1+a^2} \right|^2 \left(e^{-2\mathrm{Im}\Delta_+ z} + |a|^4 e^{-2\mathrm{Im}\Delta_- z} + 2\mathrm{Re}\{a^2 e^{i(\Delta_- - \Delta_+^*)z}\} \right) \tag{13}$$

The last term inside the bracket in (13) is oscillatory and can be neglected when the phase is large $\phi = \mathrm{Re}\{\Delta_- - \Delta_+^*\}z \gg 1$, corresponding to situations where a large number of oscillations occur within the propagation length z.

The expression for the survival probability (13) breaks down when $a^2 = -1$ or, equivalently, when

$$\mu^2 = \frac{\omega_\mathrm{P}^2}{(1 \pm i\chi)^2}. \tag{14}$$

This is the point in phase space where the photon and hidden photon are exactly degenerate. As the imaginary and real parts of μ^2 satisfy

$$\mathrm{Im}\{\mu^2\} > \mathrm{Re}\{\mu^2\} \qquad \text{for} \qquad \mathrm{Re}\{\mu^2\} > 0 \ , \tag{15}$$

the condition (14) can only be satisfied for values of $\chi \sim \mathcal{O}(1)$. In this paper we restrict ourselves to considering small values of χ, which are not only more realistic from the theoretical point of view but also are not excluded by laboratory experiments. Therefore we are always far from the resonance.

In the small mixing regime $\chi \ll 1$ a simpler formula for the photon survival probability (13) can be obtained. Expanding (10) and (11) around $\chi = 0$ we find

$$m_+^2 = \omega_{\mathrm{P}}^2 \left(1 + a\chi\right) \quad ; \quad m_-^2 = \mu^2 \left(1 - a\chi\right) \tag{16}$$

$$a \quad = \frac{\mu^2}{\omega_{\mathrm{P}}^2 - \mu^2}\chi \tag{17}$$

So that the photon survival probability becomes

$$P_{\gamma\to\gamma}(z) = 1 - 2\mathrm{Re}\{a^2\} - \chi\frac{z\omega_P^2}{\omega}\mathrm{Im}\{a\} + 2\mathrm{Re}\{a^2 e^{-iz(\omega_P^2-\mu^2)/2\omega}\} + \mathcal{O}(\chi^4). \tag{18}$$

The last term in this expression is exponentially damped and when the distances under consideration satisfy $z\mathrm{Im}\{\mu^2\} \gg 2\omega$ it can be safely neglected.

As mentioned in the introduction the inclusion of the hidden photon is not necessary for the existence of MCPs but it certainly provides one of the few natural theoretical explanations of the small mini-charges. Use of the framework described above imposes no restriction on the origin of MCPs because the hidden photon field can be consistently decoupled by formally sending $e_h \to 0$ whilst keeping ϵ constant. This can be seen directly from the Lagrangian (4) where the only term that connects the hidden photon to the other fields is proportional to e_h§. Note that m_+^2 is a constant in this limit but $\chi\mu^2$ and μ^2 vanish and therefore the mixing parameter a also tends to zero. When the hidden photon decouples the photon survival probability becomes simply

$$P = e^{-2\mathrm{Im}\Delta_+ z}. \tag{19}$$

3. Using the Sunyaev-Zel'dovich effect to constrain MCPs

As discussed in the introduction, magnetic fields exist in clusters of galaxies. As light from the CMB traverses these fields the properties of this light can be affected by the real and virtual production of MCPs. Clusters of galaxies are some of the largest objects in the universe; a typical cluster contains $\sim 10^3$ galaxies in a region ~ 2 Mpc in radius. The magnetic fields of these clusters are relatively well understood [38], and it is common to model these magnetic fields as being made up of a large number of equally sized magnetic domains. Within each domain the magnetic field is constant, and the magnitude of the magnetic field strength is constant over the whole cluster, but within each domain the

§ This decoupling can also be seen in the matrix form of the equations of motion (5). As μ^2 equals e_h^2 multiplied by some function $f(\epsilon)$ the $A-A$ matrix element is $\propto \chi^2 e_h^2 f(\epsilon) = \epsilon^2 e^2 f(\epsilon)$ and will stay constant in the decoupling limit, however the $A-B$ element is $\propto \chi e_h^2 f(\epsilon) = e_h \epsilon e f(\epsilon)$ and vanishes as $e_h \to 0$.

direction of the magnetic field vector is essentially a random variable. Photons passing through such clusters may interact with the cluster magnetic field and convert into real or virtual MCPs. This loss of photons would look like a contribution to the SZ effect of the form

$$\frac{\Delta T}{T} = \frac{1-e^{-x}}{x}\frac{\Delta I}{I_0}, \tag{20}$$

where I_0 is the photon flux from the CMB, ΔI is the flux decrement due to MCPs and $x = \omega/T_{CMB}$, and T_{CMB} is the temperature of the CMB radiation today. The best constraints would come from a cluster for which both the SZ effect and the properties of its magnetic field have been directly measured. This is uniquely the case for the Coma cluster (Abell 1656) which lies at a redshift $z = 0.023$. The properties of the Coma cluster will be discussed further in Section 3.1.

In order to constrain the MCP contribution to the SZ effect we must compute the flux deficit induced as the photons propagate through a large number of randomly oriented magnetic domains. As the CMB is a *very* non compact source, light from the CMB takes many different paths through the random magnetic field of a galaxy cluster and we need only compute the effects of MCP production averaged over this large class of paths.

We will assume that the size of a magnetic domain is sufficiently large that the final term in the photon survival probability (18) can be neglected. This is consistent whenever $\mathrm{Im}\{\mu^2\} \gg 2\omega/L$, where L is the size of the domain. Then the photon survival probability can be written as $P_i(z) = 1 - p_i - q_i z$ for $i = \|, \perp$, where $p = 2\mathrm{Re}\{a^2\}$, $q = \chi\omega_P^2 \mathrm{Im}\{a\}/\omega$. a is given by (11). To evolve the system through the cluster we will need to average over the two angles θ_n and ψ_n that determine the direction of the magnetic field in the n-th domain. The average over ψ_n, the angle of inclination of the magnetic field to the direction of motion of the photons, we will absorb into a conservative order of magnitude estimate for B. Letting θ_n be the orientation of the magnetic field in the plane perpendicular to the direction of motion of the photons, the photon components at the start of the $(n+1)$-th domain are related to those at the start of the n-th domain by‖

$$\begin{pmatrix} A_x \\ A_y \end{pmatrix}_{n+1} = \left[\left(1 - \frac{\delta_{n1}\langle p\rangle + \langle q\rangle L}{2}\right)\mathbb{1} + \frac{\delta_{n1}dp + dqL}{2}\begin{pmatrix} \cos 2\theta_n & \sin 2\theta_n \\ \sin 2\theta_n & -\cos 2\theta_n \end{pmatrix}\right]\begin{pmatrix} A_x \\ A_y \end{pmatrix}_n \tag{21}$$

where $\langle q\rangle = (q_\perp + q_\|)/2$ and $dq = (q_\perp - q_\|)/2$, with equivalent definitions for $\langle p\rangle$ and dp. Assuming that, on average, $\cos^2\theta_n = \sin^2\theta_n = 1/2$ and $\cos\theta_n = \sin\theta_n = 0$ it can be shown that after passing through N magnetic domains the average photon flux I_N, is related to the initial photon flux, I_0, by

$$I_N = I_0\Big(1 - \langle p\rangle - N\langle q\rangle L + \mathcal{O}(N^2\langle q\rangle^2)\Big). \tag{22}$$

Combining equations (20) and (22) we can constrain the CMB temperature anisotropies induced in MCP models to be less than those of the SZ effect.

‖ In principle the propagation is described by a 4×4 matrix. However, after the initial damping only the V_+ eigenmodes survive and we can use effectively a 2×2 description.

In the general case we compute the photon survival probabilities numerically, but there are two limits which can be understood analytically. If the plasma frequency is sufficiently large $\omega_{\rm P}^2 \gg |\mu^2|$, the imaginary part of the mass of the photon like state (+) is well approximated by $\mathrm{Im}\{m_+^2\} = \chi^2 \mathrm{Im}\{\mu^2\} = -\epsilon^2 e^2 \kappa \omega$. This regime is equivalent to the decoupling of the hidden photon discussed in Section 2 ($e_h \to 0$, $\mu^2 \to 0$ but $\chi^2\mu^2 =$ constant). In this regime the mixing angle a is suppressed not only by χ but also by the ratio $\mu^2/\omega_{\rm P}^2$ and the photon survival probability is simply

$$P(\gamma \to \gamma) = 1 - z\epsilon^2 e^2 \kappa + \mathcal{O}(a^2). \tag{23}$$

So $\langle p \rangle = 0$ and $\langle q \rangle = \epsilon^2 e^2 \langle \kappa \rangle$ in (22).

In the opposite limit, $|\mu^2| \gg \omega_{\rm P}^2$, the situation also simplifies, recovering the expressions derived in [23]. The mixing angle is only suppressed by χ and is real in the limit $\omega_{\rm P} \to 0$. The mass of the photon like state (+) still has an imaginary part, but this is suppressed by the small quantity $\omega_{\rm P}^2/|\mu^2|$,

$$\mathrm{Im}\,\{m_+^2\} \simeq \chi^2 \mathrm{Im}\,\{\mu^2\} \frac{\omega_{\rm P}^4}{|\mu^2|^2} = \omega \epsilon^2 e^2 \kappa \frac{\omega_{\rm P}^4}{|\mu^2|^2}. \tag{24}$$

In this limit the photon survival probability is

$$P(\gamma \to \gamma) \simeq 1 - 2\chi^2 - 4\chi^2 \frac{\omega_P^2 \mathrm{Re}\{\mu^2\}}{|\mu^2|^2} - \chi^2 \frac{z\omega_P^2 \mathrm{Im}\{\mu^2\}}{\omega |\mu^2|^2} + \mathcal{O}\left(\frac{\omega_P^4}{|\mu^2|^2}\right). \tag{25}$$

In the limit $\omega_{\rm P} \to 0$ the photon survival probability becomes constant

$$\lim_{\omega_{\rm P} \to 0} P(\gamma \to \gamma) \simeq 1 - 2\chi^2. \tag{26}$$

So $\langle p \rangle = 2\chi^2$ and $\langle q \rangle = 0$ in (22). This can be understood by considering equation (12). In the $\omega_{\rm P} \to 0$ limit, $a \to -\chi$ and an initial photon state is mainly V_+ with a very small (proportional to χ^2) component of V_-. In this case, the V_- state is the original hidden photon $\tilde{B}_\mu$ which, by definition, is the state that couples to the hidden sector particles. Therefore only the V_- component of the initial state can be damped by pair production of MCPs and after traveling distances $z \gtrsim 2\omega \ln(\chi)/\mathrm{Im}\{\mu^2\}$ the final state is $V_+/(1+\chi^2)$. Squaring the amplitude of this gives the photon survival probability (26).

3.1. Constraints from the Coma cluster

The most detailed information about the strength and structure of the magnetic fields in clusters of galaxies typically comes from measurements of Faraday rotation of light at radio frequencies. The presence of a magnetic field in an ionized plasma, such as the intracluster medium, sets a preferred direction for the gyration of electrons, leading to a difference in the index of refraction for left and right circularly polarized radiation as it passes through the plasma. This is equivalent to a rotation of the plane of polarization of linearly polarized light, known as the Faraday rotation, which depends on the thermal electron density and the magnetic field strength. By taking Faraday rotation measurements of an entire cluster, not only the magnetic field strength, but also its coherence length, can be estimated. It has been shown [16, 17], however, that the interactions of photons and mini-charged particles in a transverse magnetic field also lead to the rotation of polarization, and these effects are

expected to be strongest at low frequencies. Therefore it is unclear whether the magnetic field strengths calculated from Faraday rotation measurements can be reliably used in the computation of CMB temperature anisotropies due to MCPs.

Faraday rotation is not, however, the only way to estimate the magnetic field strength of a cluster. For the Coma cluster a hard X-ray flux has been measured exceeding the thermal emission. This has its origin in the inverse Compton scattering of photons by relativistic electrons which are accelerated by the magnetic field of the galaxy cluster. This inference of the magnetic field is not based on subtle polarization measurements and therefore we expect it to be essentially free of contamination by MCPs. Hard X-ray observations of the Coma cluster imply a magnetic field strength of 0.16×10^{-10} T [39, 40], roughly an order of magnitude smaller than that inferred from Faraday rotation measurements [41]. Whilst, within the Standard Model, it is thought that these two sets of observations can be reconciled by more realistic cluster models [42]. The size of a magnetic domain can be estimated from images of the Faraday rotation of the Coma cluster, $L \approx 10$ kpc, [41] and the size of these correlations will not be affected by mixing with MCPs.

We note that it would be possible to derive constraints on MCP models by requiring that the MCP induced rotation of linearly polarized light at radio frequencies be less than the measured Faraday rotation [41]. However these constraints are subsumed by the constraints coming from measurements of the SZ effect, which we focus on for the remainder of this article.

To compute the contribution of MCPs to the SZ effect we also need to know the electron density in the intracluster plasma. This can be inferred, for the Coma cluster, from soft X-ray measurements taken during the ROSAT all sky survey [43]. From these observations it is inferred that $n_e = 2.89 \times 10^{-3}$ cm^{-3} in the core of the cluster and $n_e \approx 1 \times 10^{-3}$ cm^{-3} away from the core. This corresponds to a plasma frequency of $\omega_P \approx 10^{-12}$ eV.

The SZ effect of the Coma cluster has been measured precisely in a number of frequency bands [44], as shown in Table 1. For each observation we constrain the temperature

Instrument		Temperature Decrement	Observational Frequency
OVRO	[45]	$\Delta T = -520 \pm 83$ μK	32.0 GHz
WMAP	[46]	$\Delta T = -240 \pm 180$ μK	60.8 GHz
WMAP	[46]	$\Delta T = -340 \pm 180$ μK	93.5 GHz
MITO	[47]	$\Delta T = -184 \pm 39$ μK	143 GHz
MITO	[47]	$\Delta T = -32 \pm 79$ μK	214 GHz
MITO	[47]	$\Delta T = 172 \pm 36$ μK	272 GHz

Table 1. SZ observations of the Coma Cluster

decrement due to production of MCPs with the largest measured temperature decrement within 2σ error bars. All the observations detailed above give constraints on the parameters of the MCP model of the same order of magnitude, with those by MITO at 214 GHz, being

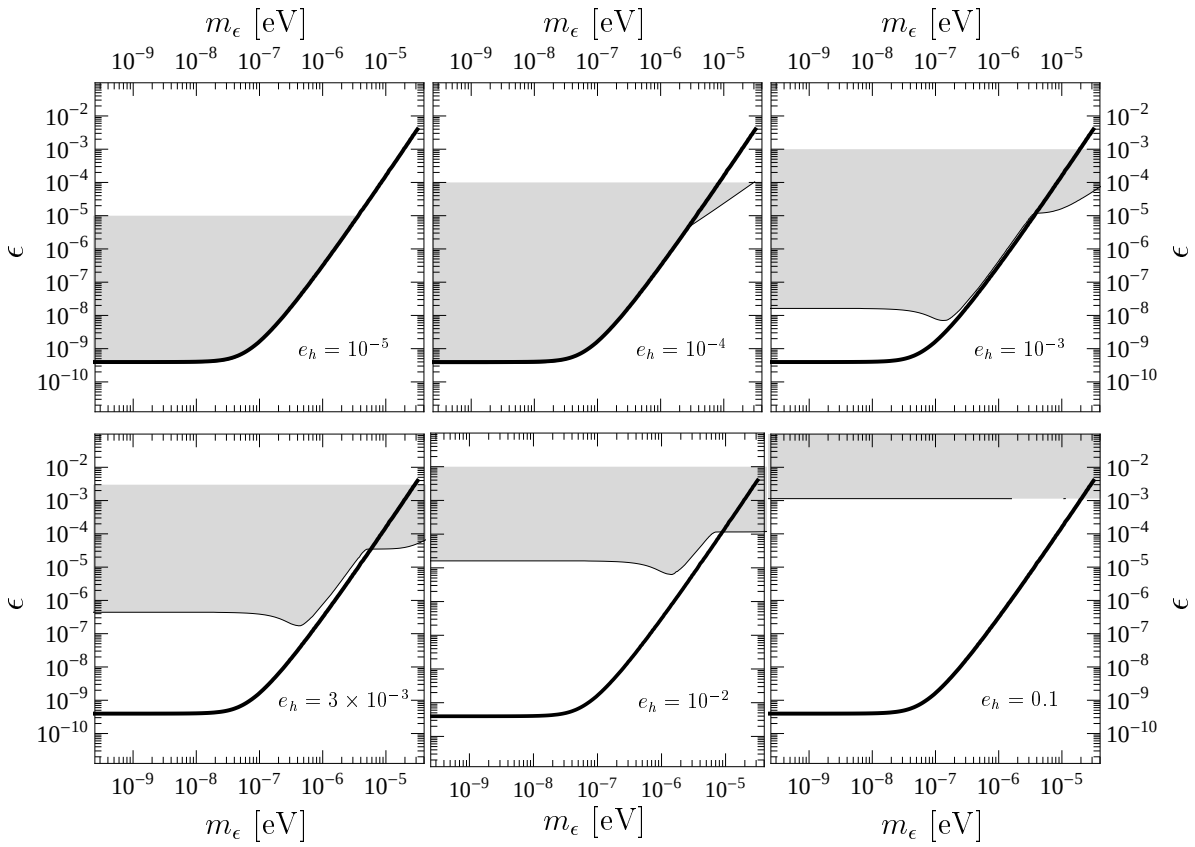

Figure 2. The constraints of the SZ effect on MCPs. The solid black line shows the upper bound in the mini-charge, MCP mass phase space on models which contain MCPs but no hidden photons (we consider a Dirac fermion, but scalars are very similar). The gray region shows the excluded region for models which include hidden photons. The different plots show different values of the hidden sector gauge coupling, given in units of the electric charge.

the most constraining. The numerical bounds quoted below come from this measurement.

To calculate the constraints on MCPs from the SZ measurements of the Coma cluster we assume that in most of the volume of the Coma cluster $B \approx 1 \times 10^{-11}$ T, which estimate includes an averaging over the angles ψ_n, and that the size of a magnetic domain is $L \approx 10$ kpc. The cluster magnetic fields extend out to a radius of at least 1 Mpc, so we assume that light from the CMB traverses approximately 100 domains. We take the average plasma frequency to be $\omega_P = 10^{-12}$ eV. The MCP induced temperature anisotropies (20) at $\nu \sim 214$ GHz are, from (22), constrained to be

$$\frac{\Delta T}{T} = 0.25\Big(\langle p\rangle + NL\langle q\rangle\Big) < 7.0 \times 10^{-5}. \tag{27}$$

Our assumption that the last term in (18) can be safely neglected when calculating the survival probability in each domain of the Coma cluster means that our constraints are valid for $\mathrm{Im}\{\mu^2\} \gg 2\omega/L$, which for observations at 214 GHz implies $\mathrm{Im}\{\mu^2\} \gg 1.1 \times 10^{-30}$ eV^2.

The constraints this imposes on the charge and mass of MCPs are shown in Figure 2. The upper bound on models without hidden photons is shown as a solid line. The gray regions are those excluded for models which include both hidden sector photons and MCPs.

The upper bound on these regions comes from requiring that $\chi \equiv \epsilon e/e_h < 1$. The excluded region in the (m_ϵ, ϵ) plane for models with hidden photons varies significantly with e_h. For small values of the hidden sector gauge coupling the constraints are indistinguishable from those of the pure MCP case. This is the $|\mu^2| \ll \omega_{\rm P}^2$ limit discussed in the previous section. For larger gauge couplings the constraints on the mini-charge are much weaker because in this region of the parameter space only the hidden photon component of the initial state is damped by the production of MCPs. This corresponds to the $|\mu|^2 \gg \omega_P^2$ limit.

In certain regions of the parameter space it is possible to understand these limits analytically. When the adiabatic parameter is large $\lambda \gg 1$ an analytic expression for the complex refractive index exists. For light at 214 GHz passing through the magnetic fields of the Coma cluster large adiabatic parameter corresponds to

$$\epsilon^{1/3} \gg 1.1 \times 10^4 \left(\frac{m_\epsilon}{\rm eV}\right). \tag{28}$$

and this corresponds to the region on the left of Figure 2 where the constraints are independent of the MCP mass.

When the adiabatic parameter is large and $|\mu|^2 \ll \omega_P^2$, corresponding to $e_h \epsilon^{1/3} \ll 7 \times 10^{-8}$, the hidden photons effectively decouple. The photon survival probability is given by (23) and measurements of the SZ effect in the Coma cluster constrain

$$\epsilon < 4 \times 10^{-10}. \tag{29}$$

In the alternative limit $|\mu|^2 \gg \omega_P^2$ the photon survival probability is given by (26) and measurements of the SZ effect constrain

$$\chi < 1 \times 10^{-2}, \tag{30}$$

or equivalently

$$\epsilon < 3 \times 10^{-2} e_h. \tag{31}$$

3.2. Hyperweak hidden gauge couplings

Above we have seen that our bounds are strongest for mini-charged particles without hidden photons and for very small hidden sector gauge couplings. Although the first case is interesting in itself, let us also briefly motivate the case of small hidden sector gauge couplings. Indeed we will see below that our bounds start to penetrate a theoretically very interesting region.

Hyperweak gauge interactions [48] are a typical feature in so-called LARGE volume scenarios in string theory. In LARGE volume scenarios the string scale M_s is related to the Planck scale M_P (and the string coupling g_s) via

$$M_P^2 = \frac{4\pi}{g_s^2} \mathcal{V} M_s^2, \tag{32}$$

with a LARGE volume $\mathcal{V} = V_6 M_s^6$ of the six compactified dimensions. Due to the LARGE volume the string scale can now be much lower than the Planck scale. For example for a volume of the order of $\mathcal{V} \sim 10^{12}$ one obtains a string scale $M_s \sim 10^{11}\,{\rm GeV}$. This scale is particularly interesting in scenarios where a supersymmetry breaking of size $\sim M_s^2$ is

mediated to the Standard Model by gravity resulting in masses for the superpartners of the order of $\sim M_s^2/M_P \sim 1\,\mathrm{TeV}$. For an even larger volume $\mathcal{V} \sim 10^{27}$ the string scale itself could be as low as a TeV.

In the LARGE volume scenarios gauge groups live on D7 branes with 7+1 dimensions. The extra 4 space dimensions are removed by wrapping the brane around a cycle in the extra dimensions. The gauge coupling is then given by

$$g^2 = \frac{2\pi g_s}{\mathcal{V}_4} \sim \frac{2\pi g_s}{\mathcal{V}^{\frac{2}{3}}}, \tag{33}$$

where $\mathcal{V}_4 = V_4 M_s^4$ is the volume of the compactified 4 extra dimensions of the brane. In the last step we have assumed that the brane extents through most of the LARGE volume and the latter has roughly the same extent in all directions. In this case the gauge coupling will be very small. (The Standard Model gauge groups live on smaller cycles or singularities and accordingly have larger gauge couplings ~ 1.) Typical values for these hyperweak gauge couplings are of the order

$$e_h \sim \begin{cases} 10^{-4} & \sim 10^{-3}\, e \quad \text{for} \quad \mathcal{V} \sim 10^{12} \\ 10^{-10} & \sim 10^{-9}\, e \quad \text{for} \quad \mathcal{V} \sim 10^{27} \end{cases} . \tag{34}$$

This is exactly the regime where our bound is most constraining.

Finally, let us also take a brief look at the kinetic mixing in these scenarios (cf. [14] for details). An estimate of the kinetic mixing between a visible sector (non-hyperweak) U(1) and a hidden hyperweak U(1) gauge group yields,

$$\chi \sim \frac{e e_h}{6\pi^2}. \tag{35}$$

Accordingly we find for the mini-charge

$$|\epsilon| = \left|\frac{e_h \chi}{e}\right| \sim \frac{e_h^2}{6\pi^2} \sim \begin{cases} \text{few} \times 10^{-10} & \text{for} \quad \mathcal{V} \sim 10^{12} \\ \text{few} \times 10^{-20} & \text{for} \quad \mathcal{V} \sim 10^{27} \end{cases} . \tag{36}$$

Comparing with Fig. 2 we see that our bound probes the region of interest for the scenario with a string scale $M_s \sim 10^{11}\,\mathrm{GeV}$. We have summarized this in Fig. 3 where we have also included bounds from laboratory searches and low density/temperature bounds from cosmology. The solid line shows the edge of the excluded region for models with only mini-charged particles. If the strength of the magnetic field and the plasma frequency are assumed to be the same in each magnetic domain in the cluster, for models with hidden photons and hyperweak hidden gauge couplings satisfying (36) there are 'holes' in the excluded region. However if small fluctuations in the magnetic field strength and plasma frequency are allowed, and such fluctuations would naturally be expected to occur in the galaxy cluster, these holes are closed and the entire region above the solid line is excluded.

4. The ISW effect: A future test

On the largest scales on the sky ($\theta > 1^\circ$) the dominant source of secondary anisotropies of the CMB is not the SZ effect but the Integrated Sachs-Wolfe effect (ISW) [2]. The ISW effect occurs when gravitational potentials evolve with time, as then the blue-shifting of a photon falling into the gravitational well is not exactly canceled by the red-shifting of

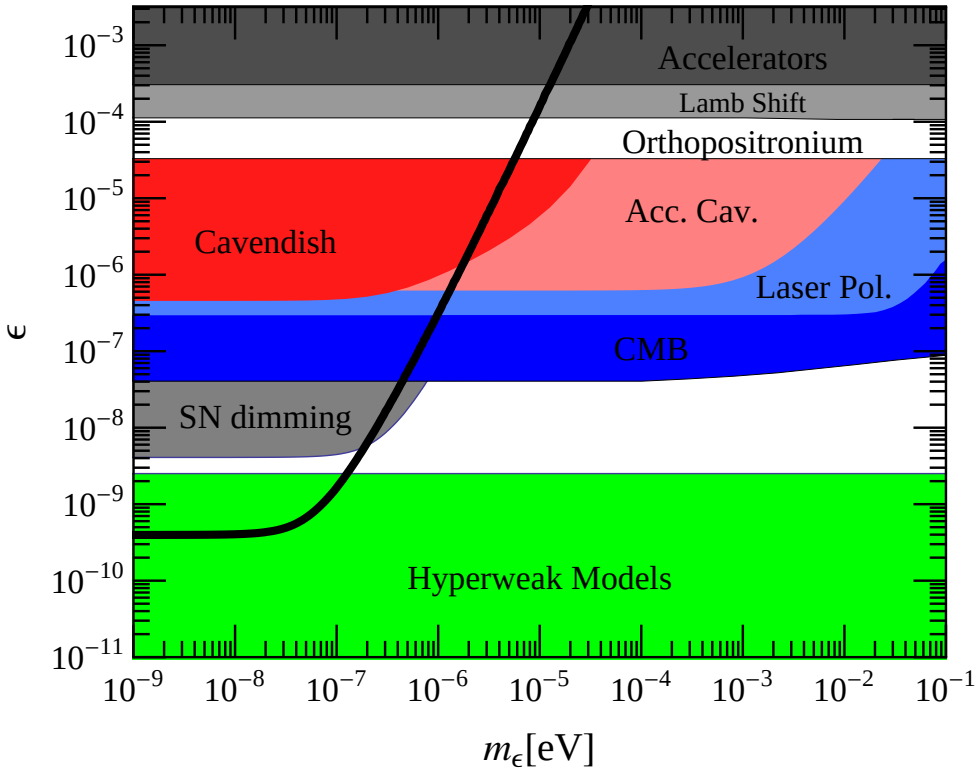

Figure 3. Bounds on mini-charged particles for very weak hidden sector gauge couplings. They apply also to models with only mini-charged particles. The solid black line shows the upper bound on the mini-charge obtained in this paper from the SZ effect. The green area is a prediction in LARGE volume scenarios in string theory with a hyperweak U(1) and a string scale $M_s \lesssim 10^{11}\,\mathrm{GeV}$. For comparison, we have also included bounds arising from accelerators [25,26], Lamb shift [49], positronium decays [50], tests of Coulomb's Law [51], accelerator cavities [52], laser polarization experiments [24], the CMB [28] and supernova dimming [29]. All these bounds arise from physics occurring in low density/temperature regions.

the photon climbing out of the potential well, and there is a net effect on the energy of a photon,

$$\frac{\Delta T}{T} \approx -2 \int \dot{\Phi} d\tau, \tag{37}$$

where Φ is the gravitational potential along a line of sight, and a dot denotes differentiation with respect to conformal time, τ.

If the universe is close to being flat most of the late time ISW effect is caused by dark energy, and observations of the ISW effect have been used to probe its properties. However measuring the ISW effect is not easy as the signal is a fraction of the size of the primordial CMB anisotropies. It can be extracted, however, by looking for correlations between the CMB temperature fluctuations and tracers of the density of matter. These correlations have been detected using a variety of density probes and over a wide range of the electromagnetic spectrum [3].

The ISW effect dominates on the very largest scales, those of superclusters of galaxies which can stretch over distances of tens of mega-parsecs. We would expect mini-charged particles to be constrained by observations of the ISW effect only if there exist magnetic fields in galaxy superclusters. So far no detailed study has been done of the magnetic fields on such scales, however there are some hints that magnetic fields exist in these environments from observations of the diffuse radio emission from large scale networks of galaxies [53]. Also if the magnetic fields in galaxies are produced during structure formation (as opposed to having their origin in a primordial magnetic field) then simulations show that magnetic fields should indeed exist in superclusters of galaxies (e.g. [54]).

It is to be hoped that as we continue to learn more abut the magnetic fields in super clusters of galaxies we will be able to use measurements of the ISW effect to constrain the properties of mini-charged particles. The magnetic fields in these structures are expected, from simulations, to be of the same order of magnitude as those in galaxy clusters and so we expect to be able to significantly improve our bounds, both because the temperature fluctuations in the CMB due to the ISW effect are much smaller $\Delta T/T \sim 10^{-6}$ than those of the SZ effect, and also because the distances traveled through the magnetic fields of superclusters of galaxies are greater than the equivalent distances used in the SZ calculation.

5. Conclusions

Mini-charged particles arise in a variety of extensions to the Standard Model, most naturally in models which also contain hidden photons. In such models the propagation of photons in a transverse magnetic field is affected by the real and virtual production of MCPs. MCPs can be constrained by a wide variety of terrestrial, astrophysical and cosmological experiments. However some of these constraints, those coming from processes occurring in dense environments such as the interior of stars, do not constrain all available MCP models. Therefore it is necessary to have alternative probes of this region of parameter space which require only physics in low density/temperature environments. Such constraints are particularly relevant for upcoming laboratory searches for MCPs.

In this article we have developed such a new test for MCPs from observations of the Sunyaev-Zel'dovich effect. As photons from the CMB pass through the magnetic fields of galaxy clusters some photons are lost due to the production of MCPs and this decrement in the photon flux appears as an additional contribution to the SZ effect. Insisting that this flux decrement is not larger than the observed SZ effect constrains new regions of the MCP parameter space. Our bounds are most constraining for models of MCPs without hidden sector photons, and for models with small hidden sector gauge coupling which are well motivated in the LARGE volume string scenario.

If, in the future, new observations lead us to a better understanding of the magnetic fields in the largest scale structures in the universe, a similar test could be made with observations of the ISW effect, which have the prospect to be even more constraining for MCP models.

Acknowledgments

We would like to thank Mark Goodsell for valuable discussions and collaboration on related subjects.

References

[1] J. E. Carlstrom, G. P. Holder, and E. D. Reese, *Cosmology with the Sunyaev-Zel'dovich Effect*, *Annual reviews in Astronomy and Astrophysics* **40** (2002) 643–680, [astro-ph/].

[2] R. K. Sachs and A. M. Wolfe, *Perturbations of a cosmological model and angular variations of the microwave background*, *Astrophys. J.* **147** (1967) 73–90.

[3] T. Giannantonio *et. al.*, *Combined analysis of the integrated Sachs-Wolfe effect and cosmological implications*, *Phys. Rev.* **D77** (2008) 123520, [arXiv:0801.4380].

[4] B. Holdom, *Two U(1)'s and Epsilon Charge Shifts*, *Phys. Lett.* **B166** (1986) 196.

[5] F. Brummer, J. Jaeckel, and V. V. Khoze, *Magnetic Mixing – Electric Minicharges from Magnetic Monopoles*, *JHEP* **06** (2009) 037, [arXiv:0905.0633].

[6] S. A. Abel, J. Jaeckel, V. V. Khoze, and A. Ringwald, *Illuminating the hidden sector of string theory by shining light through a magnetic field*, *Phys. Lett.* **B666** (2008) 66–70, [hep-ph/0608248].

[7] S. A. Abel, M. D. Goodsell, J. Jaeckel, V. V. Khoze, and A. Ringwald, *Kinetic Mixing of the Photon with Hidden U(1)s in String Phenomenology*, *JHEP* **07** (2008) 124, [arXiv:0803.1449].

[8] K. R. Dienes, C. F. Kolda, and J. March-Russell, *Kinetic mixing and the supersymmetric gauge hierarchy*, *Nucl. Phys.* **B492** (1997) 104–118, [hep-ph/9610479].

[9] A. Lukas and K. S. Stelle, *Heterotic anomaly cancellation in five dimensions*, *JHEP* **01** (2000) 010, [hep-th/9911156].

[10] D. Lust and S. Stieberger, *Gauge threshold corrections in intersecting brane world models*, *Fortsch. Phys.* **55** (2007) 427–465, [hep-th/0302221].

[11] S. A. Abel and B. W. Schofield, *Brane-antibrane kinetic mixing, millicharged particles and SUSY breaking*, *Nucl. Phys.* **B685** (2004) 150–170, [hep-th/0311051].

[12] R. Blumenhagen, G. Honecker, and T. Weigand, *Loop-corrected compactifications of the heterotic string with line bundles*, *JHEP* **06** (2005) 020, [hep-th/0504232].

[13] R. Blumenhagen, S. Moster, and T. Weigand, *Heterotic GUT and standard model vacua from simply connected Calabi-Yau manifolds*, *Nucl. Phys.* **B751** (2006) 186–221, [hep-th/0603015].

[14] M. D. Goodsell, J. Jaeckel, J. Redondo, and A. Ringwald, *Naturally light hidden photons in LARGE volume string compactifications*, *DESY 09-123; DCPT/09/124; IPPP/09/62* [arXiv:0909.0515].

[15] B. Batell and T. Gherghetta, *Localized U(1) gauge fields, millicharged particles, and holography*, *Phys. Rev.* **D73** (2006) 045016, [hep-ph/0512356].

[16] H. Gies, J. Jaeckel, and A. Ringwald, *Polarized light propagating in a magnetic field as a probe of millicharged fermions*, *Phys. Rev. Lett.* **97** (2006) 140402, [hep-ph/0607118].

[17] M. Ahlers, H. Gies, J. Jaeckel, and A. Ringwald, *On the particle interpretation of the PVLAS data: Neutral versus charged particles*, *Phys. Rev.* **D75** (2007) 035011, [hep-ph/0612098].

[18] **BFRT** Collaboration, R. Cameron *et. al.*, *Search for nearly massless, weakly coupled particles by optical techniques*, *Phys. Rev. D* **47** (May, 1993) 3707–3725.

[19] **PVLAS** Collaboration, E. Zavattini *et. al.*, *Experimental observation of optical rotation generated in vacuum by a magnetic field*, *Physical Review Letters* **96** (2006), no. 11 110406.

[20] **Q & A** Collaboration, S.-J. Chen, H.-H. Mei, and W.-T. Ni, *Q & A experiment to search for vacuum dichroism, pseudoscalar-photon interaction and millicharged fermions*, *Mod. Phys. Lett.* **A22** (2007) 2815–2831, [hep-ex/0611050].

[21] **BMV** Collaboration, R. Battesti *et. al.*, *The BMV experiment : a novel apparatus to study the propagation of light in a transverse magnetic field*, *Eur. Phys. J. D* **46** (2008) 323, [arXiv:0710.1703].

[22] P. Pugnat *et. al.*, *Feasibility study of an experiment to measure the vacuum magnetic birefringence*, *Czech. J. Phys.* **55** (2005) A389–A397.

[23] M. Ahlers, H. Gies, J. Jaeckel, J. Redondo, and A. Ringwald, *Light from the Hidden Sector*, *Phys. Rev.* **D76** (2007) 115005, [arXiv:0706.2836].

[24] M. Ahlers, H. Gies, J. Jaeckel, J. Redondo, and A. Ringwald, *Laser experiments explore the hidden sector*, *Phys. Rev.* **D77** (2008) 095001, [arXiv:0711.4991].

[25] S. Davidson and M. E. Peskin, *Astrophysical bounds on millicharged particles in models with a paraphoton*, *Phys. Rev.* **D49** (1994) 2114–2117, [hep-ph/9310288].

[26] S. Davidson, S. Hannestad, and G. Raffelt, *Updated bounds on milli-charged particles*, *JHEP* **05** (2000) 003, [hep-ph/0001179].

[27] E. Masso and J. Redondo, *Compatibility of CAST search with axion-like interpretation of PVLAS results*, *Phys. Rev. Lett.* **97** (2006) 151802, [hep-ph/0606163].

[28] A. Melchiorri, A. Polosa, and A. Strumia, *New bounds on millicharged particles from cosmology*, *Phys. Lett.* **B650** (2007) 416–420, [hep-ph/0703144].

[29] M. Ahlers, *The Hubble diagram as a probe of mini-charged particles*, arXiv:0904.0998.

[30] Y. B. Zeldovich and R. A. Sunyaev, *The Interaction of Matter and Radiation in a Hot-Model Universe*, *Astrophys. Space Sci.* **4** (1969) 301.

[31] R. A. Sunyaev and Y. B. Zeldovich, *The Observations of relic radiation as a test of the nature of X-Ray radiation from the clusters of galaxies*, *Comments Astrophys. Space Phys.* **4** (1972) 173–178.

[32] M. Birkinshaw, *The sunyaev-zel'dovich effect*, *Physics Reports* **310** (1999), no. 2-3 97 – 195.

[33] J. E. Carlstrom, M. Joy, G. Holder, W. L. Holzapfel, S. Laroque, J. J. Mohr, and E. Reese, *The Sunyaev-Zel'dovich Effect*, in *Constructing the Universe with Clusters of Galaxies*, 2000.

[34] S. L. Dubovsky, D. S. Gorbunov, and G. I. Rubtsov, *Narrowing the window for millicharged particles by CMB anisotropy*, *JETP Lett.* **79** (2004) 1–5, [hep-ph/0311189].

[35] A.-C. Davis, C. A. O. Schelpe, and D. J. Shaw, *The Effect of a Chameleon Scalar Field on the Cosmic Microwave Background*, arXiv:0907.2672.

[36] T. Erber, *High-energy electromagnetic conversion processes in intense magnetic fields*, *Rev. Mod. Phys.* **38** (1966) 626–659.

[37] W.-y. Tsai and T. Erber, *Photon Pair Creation in Intense Magnetic Fields*, *Phys. Rev.* **D10** (1974) 492.

[38] C. L. Carilli and G. B. Taylor, *Cluster magnetic fields*, *Annual Review of Astronomy and Astrophysics* **40** (2002), no. 1 319–348.

[39] T. A. Enßlin, R. Lieu, and P. L. Biermann, *Non-thermal origin of the EUV and HEX excess emission of the Coma cluster - the nature of the energetic electrons*, *Astronomy and Astrophysics* **344** (Apr., 1999) 409–420, [astro-ph/].

[40] C. L. Sarazin, *The Energy Spectrum of Primary Cosmic-Ray Electrons in Clusters of Galaxies and Inverse Compton Emission*, *The Astrophysical Journal* **520** (Aug., 1999) 529–547, [astro-ph/].

[41] K.-T. Kim, P. P. Kronberg, P. E. Dewdney, and T. L. Landecker, *The halo and magnetic field of the Coma cluster of galaxies*, *The Astrophysical Journal* **355** (May, 1990) 29–37.

[42] L. F. G. Brunetti, G. Setti and G. Giovannini, *Particle reacceleration in the coma cluster: radio properties and hard x-ray emission*, *Monthly Notices of the Royal Astronomical Society* **320** (2001), no. 3 365–378.

[43] U. G. Briel, J. P. Henry, and H. Boehringer, *Observation of the Coma cluster of galaxies with ROSAT during the all-sky survey*, *Astronomy and Astrophysics* **259** (June, 1992) L31–L34.

[44] E. S. Battistelli *et. al.*, *Triple experiment spectrum of the sunyaev-zel'dovich effect in the coma cluster: H0*, *The Astrophysical Journal Letters* **598** (2003), no. 2 L75–L78.

[45] T. Herbig, C. R. Lawrence, A. C. S. Readhead, and S. Gulkis, *A measurement of the sunyaev-zel'dovich effect in the coma cluster of galaxies*, *The Astrophysical Journal Letters* **449** (1995), no. 1 L5–L8.

[46] **WMAP** Collaboration, C. L. Bennett *et. al.*, *First-year wilkinson microwave anisotropy probe (wmap) observations: Foreground emission*, *The Astrophysical Journal Supplement Series* **148** (2003), no. 1 97–117.

[47] M. D. Petris *et. al.*, *Mito measurements of the sunyaev-zeldovich effect in the coma cluster of galaxies*, *The Astrophysical Journal Letters* **574** (2002), no. 2 L119–L122.

[48] C. P. Burgess *et. al.*, *Continuous Global Symmetries and Hyperweak Interactions in String Compactifications*, *JHEP* **07** (2008) 073, [arXiv:0805.4037].

[49] M. Gluck, S. Rakshit, and E. Reya, *The Lamb shift contribution of very light milli-charged fermions*, *Phys. Rev.* **D76** (2007) 091701, [hep-ph/0703140].

[50] A. Badertscher *et. al.*, *An Improved Limit on Invisible Decays of Positronium*, *Phys. Rev.* **D75** (2007) 032004, [hep-ex/0609059].

[51] J. Jaeckel, *Probing Minicharged Particles with Tests of Coulomb's Law*, *Phys. Rev. Lett.* **103** (2009) 080402, [arXiv:0904.1547].

[52] H. Gies, J. Jaeckel, and A. Ringwald, *Accelerator cavities as a probe of millicharged particles*, *Europhys. Lett.* **76** (2006) 794–800, [hep-ph/0608238].

[53] J. Bagchi *et. al.*, *Evidence for Shock Acceleration and Intergalactic Magnetic Fields in a Large-Scale Filament of Galaxies ZwCl 2341.1+0000*, *New Astron.* **7** (2002) 249, [astro-ph/0204389].

[54] D. Ryu, H. Kang, and P. L. Biermann, *Cosmic Magnetic Fields in Large Scale Filaments and Sheets*, *Astronomy and Astrophysics* **335** (1998) 19–25, [astro-ph/9803275].